

Binding of the Intracellular Fas Ligand (FasL) Domain to the Adaptor Protein PSTPIP Results in a Cytoplasmic Localization of FasL^{*[5]}

Received for publication, February 28, 2005, and in revised form, September 2, 2005. Published, JBC Papers in Press, October 4, 2005, DOI 10.1074/jbc.M502222200

Wiebke Baum^{#1}, Vladimir Kirkin[‡], Sara B. Mateus Fernández[‡], Robert Pick[‡], Marcus Lettau[§], Ottmar Janssen[§], and Martin Zörnig^{#2}

From the [‡]Georg-Speyer-Haus, Paul-Ehrlich-Strasse 42-44, Frankfurt D-60596, Germany and [§]Institute of Immunology, University Hospital Schleswig-Holstein Campus Kiel, Michaelisstrasse 5, Kiel D-24105, Germany

The tumor necrosis factor family member Fas ligand (FasL) induces apoptosis in Fas receptor-expressing target cells and is an important cytotoxic effector molecule used by CTL- and NK-cells. In these hematopoietic cells, newly synthesized FasL is stored in specialized secretory lysosomes and only delivered to the cell surface upon activation and target cell recognition. FasL contains an 80-amino acid-long cytoplasmic tail, which includes a proline-rich domain as a *bona fide* Src homology 3 domain-binding site. This proline-rich domain has been implicated in FasL sorting to secretory lysosomes, and it may also be important for reverse signaling via FasL, which has been described to influence T-cell activation. Here we report the identification of the Src homology 3 domain-containing adaptor protein PSTPIP as a FasL-interacting partner, which binds to the proline-rich domain. PSTPIP co-expression leads to an increased intracellular localization of Fas ligand, thereby regulating extracellular availability and cytotoxic activity of the molecule. In addition, we demonstrate recruitment of the tyrosine phosphatase PTP-PEST by PSTPIP into FasL·PSTPIP·PTP-PEST complexes which may contribute to FasL reverse signaling.

Fas ligand (FasL³; CD95/APO-1 ligand, CD178, TNFSF6) is a 281-amino acid (aa)-long type II transmembrane molecule belonging to the large TNF family of proteins that bind to and activate members of the TNF receptor family (1, 2). FasL and its corresponding receptor Fas (CD95/APO-1) both interact as oligomers (3), and the activated Fas receptor complex initiates a proapoptotic death signal in the receptor-bearing cell (4, 5).

Although mainly known for its death-promoting activity, FasL has also been studied in the context of further nonapoptotic functions (1, 2, 6). Such experiments are motivated by the special structure of this type II transmembrane protein. In addition to its hydrophobic transmembrane domain, which anchors the molecule within the plasma membrane, and to its extracellular ectodomain, responsible for binding to its

receptor, the FasL protein possesses an 80-aa-long N-terminal intracellular part that is responsible for the transduction of (extracellular) signals into FasL-bearing cells and/or that may fulfill regulatory functions. Such a “reverse signaling” has been described in mouse T-cells, which display an altered proliferative behavior upon triggering of their FasL surface molecules (7–9). Results obtained with mouse Sertoli cells, in which FasL engagement leads to mitogen-activated protein kinase activation, as measured by an increase in Erk phosphorylation, also imply stimulatory FasL reverse signaling (10).

The importance of the intracellular domain for FasL function and regulation is underlined by its high homology among different species (7, 11, 12). Several signaling motives within the FasL intracellular domain are highly conserved, including a tandem casein kinase I phosphorylation site (aa 17–21 (11)), a phosphorylatable tyrosine at position 7, a proline-rich region (aa 40–70) with *bona fide* Src homology 3 (SH3)/WW domain-binding sites (7), and a potential nuclear localization sequence (aa 69–76).⁴ These sequence elements are likely to contribute to FasL reverse signaling and regulation, which, however, so far has only been described phenomenologically. No molecular mechanism for such signaling or for any FasL regulation involving the intracellular ligand domain has been identified.

Apart from transducing signals into the ligand-expressing cell, the intracellular FasL domain may be involved in other regulatory processes. Interestingly, FasL is not expressed ubiquitously on the surface of hematopoietic cells (*e.g.* cytotoxic T-cells and NK-cells) but is instead sorted to special organelles, the so-called secretory lysosomes, from where the molecule is delivered to the cell surface upon contact with a target cell (13). This sorting to secretory lysosomes is dependent on the proline-rich region within the intracellular FasL domain (14), but again no molecular interactors have been identified that regulate lysosomal targeting.

We screened a yeast two-hybrid library to isolate proteins that bind to the intracellular FasL domain and are involved in such processes. Here we describe the identification and analysis of the adaptor protein PSTPIP (proline, serine, threonine phosphatase-interacting protein; in this paper the human homolog CD2BP1 is for simplicity called human PSTPIP (hPSTPIP) (15, 16)) as a FasL-interacting protein, which appears to be involved in the regulation of FasL cell surface expression *versus* intracellular storage. Co-expression of PSTPIP with FasL in nonhematopoietic 293T cells leads to a decline in cell surface FasL, whereas the amount of intracellular FasL is increased. We also show that PSTPIP simultaneously interacts with the phosphatase PTP-PEST to form a ternary complex with FasL, which may be important for the phosphorylation status of PSTPIP and FasL.

^{*} This work was supported by Deutsche Forschungsgemeinschaft Grant Zo 110/2-1/2 and a grant from the Heinrich und Erna Schaufler-Stiftung. The costs of publication of this article were defrayed in part by the payment of page charges. This article must therefore be hereby marked “advertisement” in accordance with 18 U.S.C. Section 1734 solely to indicate this fact.

^[5] The on-line version of this article (available at <http://www.jbc.org>) contains supplemental Figs. S1 and S2.

¹ Present address: Institut für Normale und Pathologische Physiologie, Deutscheschhausstrasse 1-2, Marburg D-35037, Germany.

² To whom correspondence should be addressed. Tel.: 49-69-63395115; Fax: 49-69-63395297; E-mail: zoernig@em.uni-frankfurt.de.

³ The abbreviations used are: FasL, Fas ligand; aa, amino acid(s); TNF, tumor necrosis factor; SH3, Src homology 3; FACS, fluorescence-activated cell sorter; hPSTPIP, human PSTPIP; GFP, green fluorescent protein; GST, glutathione S-transferase; PIPES, 1,4-piperazine diethanesulfonic acid; BSA, bovine serum albumin; CKI, casein kinase I.

⁴ V. Kirkin, unpublished data.

EXPERIMENTAL PROCEDURES

Cell Culture and Transfections—HEK 293T, COS-1, RBL 2H3, and HeLa cell lines were grown in Dulbecco's modified Eagle's medium with 10% (v/v) fetal calf serum plus penicillin/streptavidin (Invitrogen). L12.10 mouse thymoma cells were stably transfected with *pBabe-mFasL* by electroporation and hygromycin selection in RPMI medium plus 10% fetal calf serum and penicillin/streptavidin. HEK 293T and COS-1 cells were transfected with 5–10 μ g of total plasmid DNA using Eugene reagent (Roche Applied Science) according to the manufacturer's protocol. For transient HeLa and RBL-2H3 cell transfections, 1×10^7 cells were electroporated with 20 μ g of plasmid DNA using a Gene Pulser II RF model (Bio-Rad).

Antibodies and Reagents—The polyclonal rabbit antiserum against murine PSTPIP was a gift from L. Lasky (Department of Molecular Oncology, Genentech, Inc., South San Francisco, CA) and the polyclonal rabbit antiserum against PTP-PEST from N. Tonks (Cold Spring Harbor Laboratory, Cold Spring Harbor, NY). Human PSTPIP was detected with rabbit antiserum from Carol Wise (Texas Scottish Rite Hospital for Children, Sarah M. and Charles E. Seay Center for Musculoskeletal Research, Dallas, TX) or with anti-V5 antibody (Invitrogen) and human PSTPIP lacking the SH3 domain with anti-Myc 9B11 (Cell Signaling). The anti-FLAG M2 monoclonal antibody was obtained from Sigma. Cell surface human FasL was stained for fluorescence-activated cell sorter (FACS) analysis with the anti-FasL antibody Nok-1 (Pharmingen), and total hFasL was probed in Western blot analysis with the anti-FasL antibody G-247 (Pharmingen). For immunoprecipitation of mFasL, different antibodies were used: biotinylated Mfl-3 (Pharmingen), H11 (Alexis), Alf2a (Ancell), and 3C82 (Alexis). Phosphotyrosine content of proteins was tested with the anti-Tyr(P) antibody 4G10 (Upstate Biotechnology, Inc.) in Western blot analysis. The following secondary antibodies were used for FACS analysis and immunostaining for the confocal laser-scanning microscope: anti-mouse IgG + IgM-fluorescein isothiocyanate and anti-mouse IgG1-APC (Pharmingen), anti-mouse-Alexa488, anti-rabbit-Alexa546 (both from Molecular Probes, Inc.), and anti-mouse-Alexa546 (MoBiTec).

Plasmids and Constructs—Plasmids encoding full-length and deletion mutants (lacking aa 1–39 (Δ 1–39) or aa 40–80 (Δ 40–80)) of FasL tagged with the FLAG epitope (DYKDDDDK) at the N terminus were obtained from H. Eibel (Clinical Research Unit for Rheumatology, Freiburg, Germany). Full-length murine PSTPIP (mPSTPIP) plasmids were provided by L. Lasky (Department of Molecular Oncology, Genentech, Inc., South San Francisco, CA). Plasmids coding for hPSTPIP were obtained from Carol Wise, and *PTP-PEST* cDNA was kindly provided by N. Tonks. *PTP-PEST* was subcloned into the mammalian expression vector pcDNA 3.1 (Invitrogen). To delete the hPSTPIP SH3 domain, PCR was performed using the 5' hPSTPIP-specific primer 5'-ATCGGATCCATGGCCAGGAGTACCGG-3' and the 3' hPSTPIP-specific primer 5'-ATCGAATTCTCACGCCCGGTACTCCTGGGC-3'. The resulting PCR fragment was digested with BamHI/EcoRI and subcloned into the mammalian expression vector pCMV Tag3b containing a cytomegalovirus promoter and a Myc tag (Stratagene), resulting in *pCMV CD2BP1 Δ SH3*. Two different *GFP-FasL* constructs were used; hFasL with a N-terminal FLAG tag was cloned and recombined in the Gateway vector *pDEST53* (N-terminal GFP fusion; Invitrogen). This construct was used for surface FasL analysis by FACS. hFasL cloned into *pEGFP C1* (N-terminal fusion; Clontech) was used for confocal laser-scanning microscopy. *hTNF α* , *hXIAP*, and *hHMGB1* were cloned into the pcDNA3.1 expression vector.

Yeast Two-hybrid Screening—The intracellular domain of mouse Fas ligand (aa 1–80) was cloned into the plasmid *pAS2.1* (*pAS2.1 mFasL-*

intra; Clontech) in frame with the Gal binding domain. A murine T-cell lymphoma cDNA library (MATCHMAKER; catalog no. ML4001AE; Clontech) with a diversity of 3×10^6 individual cDNA clones was used. The yeast strain Y-190 (Clontech) was sequentially transformed first with *pAS2.1 mFasL-intra* and then with the library. Prior to library screening, yeasts were tested for expression of the intracellular FasL domain by Western blot analysis. Yeast cells were plated and incubated on agar plates lacking leucine, tryptophan, and histidine for 5–10 days at 30 °C. Altogether, 6.5×10^6 transformed yeast clones were screened for FasL interaction partners. Colonies appearing were restreaked onto histidine-deficient plates and subsequently tested for β -galactosidase activity. The cDNA inserts in the *pACT* prey vector were isolated from yeast colonies with β -galactosidase activity and sequenced using standard procedures.

In Vitro Translation and Glutathione S-Transferase (GST) Pull-down—*hFasL*, *hFasL Δ 1–39*, *hFasL Δ 40–80*, *mPSTPIP*, *hPSTPIP*, and *hPSTPIP Δ SH3* were used as templates for *in vitro* transcription using T7 RNA polymerase and *in vitro* translation in the presence of 35 S-labeled methionine and rabbit reticulocyte lysate (Promega). The *in vitro* translated proteins were employed for GST pull-down assays with GST alone or with GST fusion proteins.

In Vitro Binding Assay with GST Fusion Proteins—All GST fusion constructs were subcloned into *pGEX-AHK* (Amersham Biosciences), resulting in the addition of N-terminal GST tags. GST fusion proteins were expressed in the exponentially growing *Escherichia coli* BL21C⁺ bacterial strain (Stratagene) by induction for 3 h with 1 mM isopropyl-1-thio- β -D-galactopyranoside (Roth) at 30 °C. Bacteria were harvested by centrifugation, and the fusion proteins were isolated using glutathione-Sepharose (Sigma). GST fusion proteins were incubated with the appropriate *in vitro* translated and [35 S]methionine-labeled proteins in immunoprecipitation buffer (20 mM Tris, pH 7.9, 0.02% Nonidet P-40, 10% glycerol, 100 mM NaCl, 1 mM EDTA, 4 mM MgCl₂, and 0.2 mg/ml lysozyme, 5 mM β -mercaptoethanol, 0.5 mM phenylmethylsulfonyl fluoride plus 1 freshly added tablet of Protease Inhibitor Mix Mini per 10 ml (Complete; Roche Applied Science) for 90 min at 4 °C. The beads were washed three times with 1 ml of lysis buffer, resuspended in 40 μ l of SDS sample buffer, and boiled for 5 min at 95 °C. The GST pull-down reactions were resolved by 12.5% SDS-PAGE and visualized by autoradiography.

Isolation, Purification, and Activation of Mouse T-cells from Spleen—T-lymphocytes were purified from C57Bl/6 mouse spleens with the mouse T-cell enrichment column kit (R&D Systems), according to the manufacturer's instructions. The purified cells were grown in Dulbecco's modified Eagle's medium/GlutaMax (Invitrogen), 10% fetal calf serum, 1% penicillin/streptavidin, 1% β -mercaptoethanol, and stimulated with 10 ng/ml phorbol 12-myristate 13-acetate (Calbiochem) plus 0.2 μ g/ml ionomycin (Sigma) overnight. After 18 h cells were treated with the metalloprotease inhibitor phenanthroline (1.5 mM; Sigma) to prevent shedding of FasL.

Activation of FasL by Anti-FasL Antibody—24-Well plates were coated overnight with biotinylated anti-FasL antibody Mfl-3 (2 μ g/ml). 5×10^7 L12.10 *mFasL* or L12.10 wild-type cells were added to the Mfl-3-coated wells for 0, 8, or 15 min. Cells were then lysed and used for immunoprecipitation with biotinylated Mfl-3 antibody (1 μ g/ml), followed by streptavidin-agarose.

Immunoprecipitations and Analysis of Tyrosine Phosphorylation—Transfected 293T or COS cells were lysed in 1% Triton X-100, 50 mM Hepes, pH 7.2, 10% glycerol, and 5 mM EDTA containing one protease inhibitor tablet (Complete; Roche Applied Science) plus 1 mM sodium vanadate. Some cells were pretreated with 0.1 mM pervanadate for 4 h before lysis. Immunoprecipitations were performed in vanadate-containing lysis buffer using 1

PSTPIP and Intracellular FasL Localization

$\mu\text{g/ml}$ of appropriate antibodies and prewashed protein G Dynabeads (Dyna) at 4°C overnight. The immune complexes were washed three times with lysis buffer without detergent. The proteins were then subjected to SDS-PAGE and transferred to polyvinylidene difluoride membranes (Millipore Corp.). The membranes were blocked in PBS-T (PBS, 0.05% Tween 20) containing 5% nonfat dry milk for 60 min at room temperature. Western blot analysis was performed with $1\ \mu\text{g/ml}$ affinity-purified anti-mPSTPIP, anti-PTP-PEST, anti-FasL G247.4, anti-V5, or anti-Myc 9B11 or $2\ \mu\text{g/ml}$ 4G10 anti-phosphotyrosine antibodies, followed by horseradish peroxidase-coupled secondary antibodies (Amersham Biosciences). The primary antibodies were incubated with the membrane in blocking buffer for 60 min at room temperature or overnight at 4°C . The polyclonal anti-PSTPIP and anti-PTP-PEST antibodies were used at a 1:1000 dilution in PBS-T with 5% milk. The monoclonal antibody against phosphotyrosine, 4G10-HRP, was used at a 1:1000 dilution in PBS-T with 1% bovine serum albumin (BSA). The commercial antibodies were diluted according to the manufacturers' recommendations. After incubation with the appropriate secondary antibody conjugated to horseradish peroxidase, signals were detected using ECL reagent (Amersham Biosciences).

Localization Studies of FasL and PSTPIP Using Confocal Microscopy—293T cells on coverslips were transfected with the appropriate expression constructs and fixed 48 h later with 3% formaldehyde (Roth) in PBS for 10 min, followed by permeabilization with 0.1% Triton X-100 in PBS for 5 min. Cells were washed twice in PBS plus 3% BSA, incubated with PBS plus 3% BSA for a further 20 min to block nonspecific binding of the antibody, and then stained for 1 h in PBS plus 3% BSA containing $10\ \mu\text{g/ml}$ anti-FLAG antibody M2, $1\ \mu\text{g/ml}$ anti-FasL antibody Nok-1, or a 1:40 dilution of the anti-mPSTPIP rabbit antiserum. After washing twice with PBS plus 3% BSA, cells were incubated for 60 min with a 1:1000 dilution of Alexa488 anti-mouse or Alexa546 anti-rabbit secondary antibody (Molecular Probes) in PBS plus 3% BSA. Cells were again washed in PBS plus 3% BSA and mounted in Vectashield mounting medium with 4',6-diamidino-2-phenylindole (Vector Laboratories). The samples were analyzed by confocal laser-scanning microscopy (Leica TCS SL). HeLa cells were grown on coverslips for 24 h after transfection. For fixation, they were washed once with PBS, pH 8, treated with 3% paraformaldehyde in PEM buffer (100 mM PIPES, 1 mM MgCl_2 , 1 mM EGTA, pH 6.5) for 5 min and with 3% paraformaldehyde in borate buffer (100 mM sodium borate, 1 mM MgCl_2 , pH 11) for 10 min. Cells were then permeabilized with 1% Triton X-100 in PBS, pH 8, for 15 min, washed three times with PBS-Triton (0.1% Triton X-100 in PBS, pH 8), and treated twice with NaBH_4 in PBS, pH 8 (1 mg/ml), for 10 min to reduce unreacted aldehydes. Cells were washed three times again with PBS-Triton, blocked with PBS plus 0.2% BSA for 1 h, and then incubated with anti-Myc antibody (Cell Signaling) and appropriate fluorochrome-conjugated secondary antibodies.

FACS Analysis—To quantify cell surface FasL expression, 1×10^5 cells were incubated sequentially with the anti-hFasL antibody Nok-1 in PBS plus 3% fetal calf serum (5 $\mu\text{g/ml}$) and anti-mouse IgG + IgM-fluorescein isothiocyanate or anti-mouse IgG1-APC (2.5 $\mu\text{g/ml}$) for 30 min at 4°C , washed, and analyzed using a FACSCalibur and Cell Quest Pro software (BD Biosciences).

Co-culture Killing Assay— 0.25×10^6 FasL-transfected 293T effector cells were incubated with 2.5×10^6 Fas-sensitive Jurkat A20 target cells in 2 ml of medium for 2 or 6 h at 37°C . After incubation, cells were fixed with 70% ethanol and stored at 4°C for at least 12 h. Jurkat cell death was determined by propidium iodide staining and by quantification of cells with hypoploid DNA content (sub- G_1) using FACS analysis.

RESULTS

Identification of PSTPIP as a FasL-binding Protein in a Yeast Two-hybrid Screen with the Intracellular Portion of mFasL as the Bait—To identify binding partners that interact with the intracellular FasL portion and are involved in FasL localization and/or reverse signaling, we screened a mouse thymoma cDNA library in a yeast two-hybrid screen (17) using the mouse intracellular FasL domain as the bait. One of the several clones that we isolated from the 6.5×10^6 transformants screened was the C-terminal part of the proline, serine, threonine phosphatase-interacting protein (PSTPIP) cDNA. PSTPIP was first described as an interaction partner of the phosphatase PTP-HSCF, and its functional role has been linked to the organization of the cytoskeleton (15, 18). The human PSTPIP was identified as a CD2-binding protein, hence its name CD2BP1 (16). Whereas the N terminus of PSTPIP contains an FCH (Fes/CIP-homology) domain and a coiled-coil region for protein interactions, an SH3 domain (binding to proline-rich sequences as found within the intracellular FasL domain) is localized at the PSTPIP C terminus (19). The PSTPIP deletion mutant isolated in the yeast two-hybrid screen codes for aa 130–415 and therefore includes the SH3 domain and parts of the coiled-coil region (aa 123–288 in full-length PSTPIP; see Fig. 1c).

PSTPIP Interacts *In Vitro* with the Proline-rich Region of the Intracellular FasL Domain via Its SH3 Domain—To confirm the binding of PSTPIP to FasL, which we had observed in yeast, we performed GST *in vitro* pull-down experiments. Full-length hFasL and different FasL deletion mutants were *in vitro* translated and labeled with [^{35}S]methionine. mPSTPIP was expressed and purified as a GST fusion protein, incubated with the different FasL proteins, and tested for binding by GST pull-down analysis (Fig. 1A). Whereas full-length FasL and a $\Delta 1$ –39 FasL deletion mutant (which lacks the first N-terminal 39 aa) strongly interacted with PSTPIP, the $\Delta 40$ –80 deletion mutant (lacking the proline-rich region within the intracellular FasL domain) showed only weak *in vitro* interaction. Residual binding of this mutant could be explained by the presence of a further SH3-binding site within the cytoplasmic FasL tail between aa 22 and 26. In the reverse experiment, *in vitro* translated mPSTPIP bound to the intracellular domain of mFasL fused to GST (Fig. 1B). To demonstrate that PSTPIP binds to FasL with its C-terminal SH3 domain, we used an *in vitro* translated hPSTPIP mutant lacking the SH3 domain (hPSTPIP ΔSH3) in a GST pull-down experiment. Whereas full-length hPSTPIP interacted with the intracellular domain of mFasL, the ΔSH3 mutant did not (see Fig. 1B), confirming binding of PSTPIP to FasL via a classical SH3 domain interaction (Fig. 1C). The data also demonstrate that both human and mouse FasL and PSTPIP proteins bind to each other independently of species origin, a result that is explained by the high homology between the human and murine PSTPIP SH3 sequences (93% on the protein level) and the intracellular FasL domains (76% homology).

Co-immunoprecipitation Experiments Confirm Binding of PSTPIP to FasL *In Vivo*—We used different strategies to detect *in vivo* PSTPIP/FasL interactions by co-immunoprecipitation. In the first experiments, 293T human embryonic kidney cells were transiently co-transfected with mouse PSTPIP and either with FLAG-tagged mouse or human FasL. Immunoprecipitation with an anti-FLAG antibody demonstrated co-precipitation and binding of mPSTPIP to both mouse and human FasL (Fig. 2A). In a complementary experiment, we transiently expressed FLAG-tagged mouse PSTPIP in 293–005 cells, which were stably transfected with human FasL. Again, we could show binding of PSTPIP to FasL by co-immunoprecipitation with anti-FLAG antibody (Fig. 2B). When we used untagged expression constructs, we were able

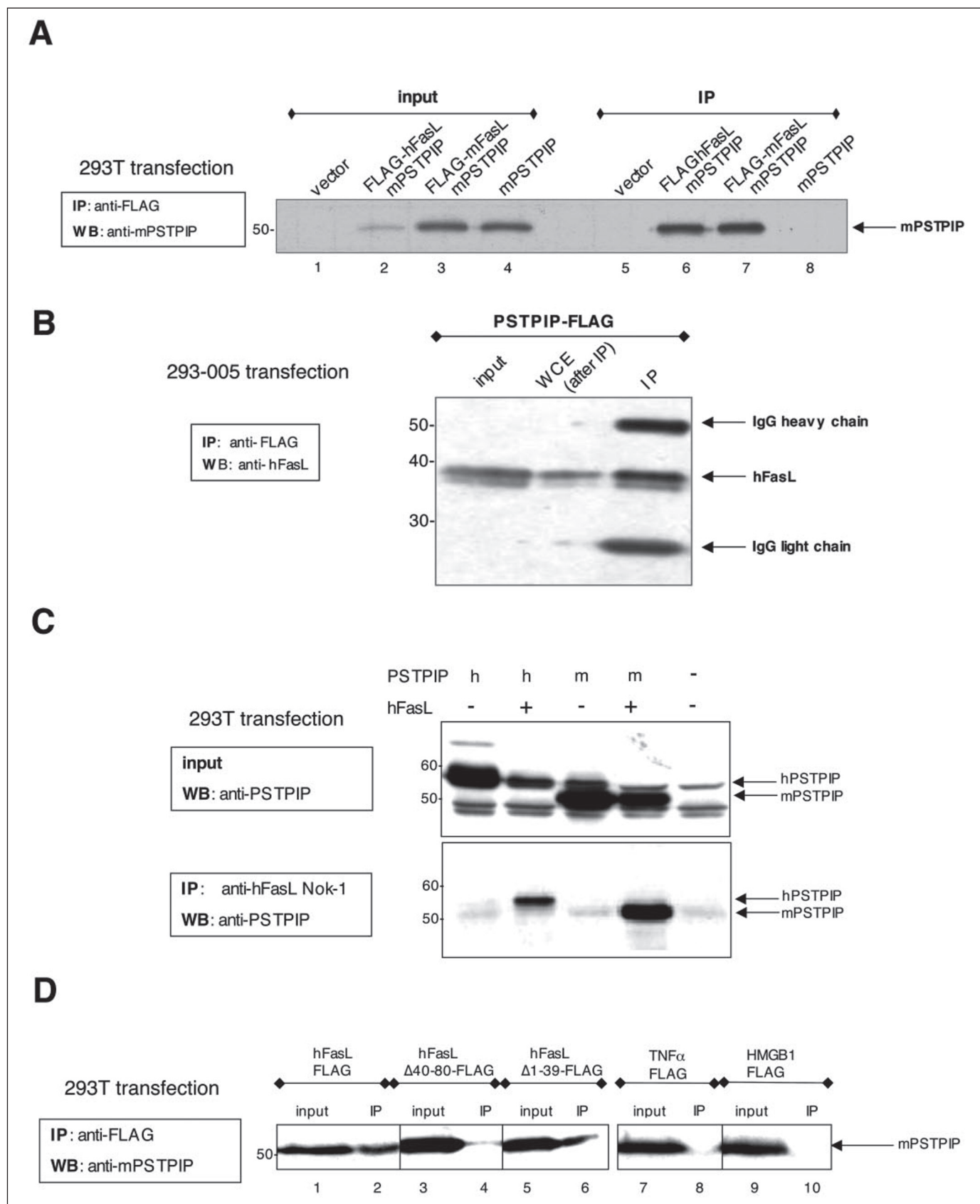


FIGURE 2. FasL and PSTPIP interact in co-immunoprecipitation experiments *in vivo*. *A*, 293T cells were transfected with *pRK-mPSTPIP* either alone or in combination with mouse (*pcDNA3.1-mFasL*) or human (*pcCR33-hFasL*) FasL, both fused to FLAG tags at their N termini. Immunoprecipitation (IP) was performed using the anti-FLAG antibody M2. mPSTPIP was co-immunoprecipitated with both mouse and human FasL, as detected by Western blot analysis (WB) with an anti-mPSTPIP antiserum. In the absence of FasL, no PSTPIP was precipitated with the anti-FLAG antibody. Input controls confirmed expression of transfected PSTPIP. The weak signal in lane 2 is explained by the low amount of lysate analyzed in this experiment. Transfections with empty vector DNA (*pcDNA3.1*) served as negative controls. *B*, 293-005 cells, which stably overexpress hFasL, were transfected with *PSTPIP-FLAG*

FLAG-tagged mouse FasL, whereas in the same experiment, mPSTPIP was efficiently precipitated together with mFasL.

We also tested the same FasL deletion mutants that we had used before in our GST pull-down analysis in co-immunoprecipitation experiments. When we co-overexpressed either full-length, $\Delta 1-39$, or $\Delta 40-80$ FLAG-FasL together with mPSTPIP in 293T cells, we were able to co-precipitate PSTPIP with full-length FasL and the $\Delta 1-39$ FasL mutant, but not with the $\Delta 40-80$ FasL version, which lacks the proline-rich region within its intracellular domain (Fig. 2D). In the control, PSTPIP was not co-immunoprecipitated with FLAG-HMGB1 or FLAG-TNF α . In some experiments, residual PSTPIP binding with the $\Delta 40-80$ FasL mutant was again observed. This may be due to the aforementioned PXXPP sequence motif present between aa 22 and 26 of FasL.

We then transfected the Fas receptor-deficient mouse thymoma cell line L12.10 with mouse FasL cDNA. After selection, we used these cells to look for binding of endogenous mPSTPIP to FasL. Because FasL expression was not stable in the L12.10 FasL cells and ceased after some time in culture, we regularly confirmed FasL expression by FACS analysis (data not shown). Before precipitating FasL from the transfected L12.10 FasL cells, we stimulated them for different lengths of time with the biotinylated anti-FasL antibody Mfl-3 to test whether the extent of PSTPIP recruitment by FasL is dependent upon FasL stimulation. Fig. 3A shows that endogenous mPSTPIP could already be co-immunoprecipitated with FasL when the cells had not been pretreated with agonistic anti-FasL antibody. Antibody stimulation of the ligand resulted in further recruitment and co-immunoprecipitation of PSTPIP with FasL, and the strongest interaction was observed after 8 min of FasL stimulation, before recruitment decreased again. This decline could be explained by a general down-regulation of the response shortly after FasL activation, but it could also be due to internalization of the FasL-antibody complex or just to antibody degradation in cell culture. Differences in the PSTPIP/FasL interaction resulting from ligand stimulation were not observed with PSTPIP-transfected 293-005 cells, which express a large amount of exogenous FasL (data not shown).

The interaction of endogenous FasL and PSTPIP was also studied in activated primary mouse T-cells. Freshly isolated mouse splenocytes were stimulated with phorbol 12-myristate 13-acetate and ionomycin for 18 h and were then used for co-immunoprecipitation experiments with different anti-mFasL antibodies. Up-regulation of both murine FasL and PSTPIP during T-cell activation has been published before (16, 20–23), although we could not demonstrate the presence of mFasL protein in the input control of our experiment, due to the lack of a suitable antibody specifically recognizing mouse FasL in Western blot analysis. However, cell surface FasL expression was confirmed by FACS analysis for the activated mouse T-cells in a parallel experiment (data not shown). The result shown in Fig. 3B reveals that endogenous mPSTPIP could be immunoprecipitated with antibodies against mFasL in activated mouse T-cells, whereas no PSTPIP/FasL interaction was seen in nonactivated control cells.

Co-localization of FasL and PSTPIP—The interaction of two molecules should be visible by their co-localization in the cell. We therefore

overexpressed PSTPIP and FLAG-FasL in HeLa cells and analyzed localization of both proteins by confocal laser-scanning microscopy. Full-length human FasL indeed co-localized with hPSTPIP (Fig. 7, *d–f*). In contrast, the $\Delta 40-80$ deletion mutant, lacking the proline-rich region within the FasL intracellular domain, did not co-localize with PSTPIP (Fig. 7, *g* and *h*). The same results were obtained in 293T cells, where full-length mouse and human FasL co-localized with mPSTPIP, in contrast to the $\Delta 40-80$ deletion mutant (supplemental Fig. 2). These results support the biochemical data suggesting that PSTPIP interacts with the proline-rich region of the intracellular FasL domain.

PSTPIP Recruits the Phosphatase PTP-PEST to FasL—PSTPIP is known to bind to the protein-tyrosine phosphatase PTP-PEST. Other PSTPIP-interacting proteins, such as WASP or c-Abl, have been shown to exist in a ternary complex with PSTPIP and PTP-PEST (16, 18, 24–26). In GST pull-down experiments, we were able to co-precipitate both *in vitro* translated PTP-PEST and FasL simultaneously with PSTPIP-GST, whereas the intracellular FasL domain fused to GST could co-precipitate PSTPIP, but (in the absence of PSTPIP) not PTP-PEST (data not shown). We then performed co-immunoprecipitation experiments in COS cells to test whether FasL also binds to PTP-PEST via the adaptor protein PSTPIP *in vivo*. Fig. 4A demonstrates that both FasL and PTP-PEST bind to the full-length PSTPIP protein, whereas only PTP-PEST interacts with the PSTPIP Δ SH3 mutant lacking the C-terminal SH3 domain, presumably via the PSTPIP coiled-coil domain, as has been published before (25). When we performed the immunoprecipitation with an anti-PTP-PEST antibody, FasL was co-precipitated only in the presence of PSTPIP (Fig. 4B). These data support a model according to which PSTPIP serves as an adaptor protein, recruiting FasL and PTP-PEST together into one complex (see Fig. 4C).

The participation of the phosphatase PTP-PEST in the formation of a ternary FasL·PSTPIP·PTP-PEST complex is likely to influence the phosphorylation status of these proteins. We therefore analyzed whether FasL and PSTPIP are subject to phosphorylation reactions *in vivo*. For this purpose, we treated transfected COS cells with the phosphatase inhibitor pervanadate and used an anti-phosphotyrosine antibody for Western blot analysis of anti-PSTPIP immunoprecipitations. As can be seen in Fig. 4A, blockage of phosphatases unmasked phosphorylation of PSTPIP and PSTPIP Δ SH3. The fact that overexpression of PTP-PEST leads to decreased PSTPIP phosphorylation even in the presence of pervanadate indicates that PTP-PEST indeed binds to and dephosphorylates PSTPIP protein. However, we were not able to demonstrate phosphorylation of FasL in COS or 293T cell overexpression systems. This may be due to the absence of kinases in these cells, which specifically phosphorylate FasL, or due to insufficient inhibition of phosphatases (*e.g.* PTP-PEST).

Co-expression of PSTPIP Leads to Decreased FasL Cell Surface Localization and Reduced FasL-mediated Target Cell Killing—In many cell types FasL is constitutively expressed at the cell surface, whereas in hematopoietic cells, the molecule is localized and stored in cytoplasmic secretory lysosomes, from where it is delivered to the cell surface upon activation of the cell (13). The intracellular domain of FasL has been shown to be responsible for this intracellular storage, and we therefore

and used for lysate preparation 48 h later. Co-immunoprecipitation with anti-FLAG antibody-coupled agarose followed by anti-hFasL Western blot analysis (G247 antibody) revealed binding of FasL to PSTPIP. Analysis of an aliquot of the "whole cell extract" (WCE (after IP)) used for immunoprecipitation (comparable in amount with the aliquot used for the input control) showed a decrease in FasL protein after immunoprecipitation of PSTPIP. In the *IP* lane, both the heavy and light chains of the mouse anti-FLAG IgG₁ antibody are visible. *C*, 293T cells were transfected with mouse (*pRK-mPSTPIP*) or human (*pcDNA3.1-hPSTPIP*) PSTPIP either alone or in combination with human FasL (*pCR33-hFasL*). Co-immunoprecipitation with the anti-hFasL antibody Nok-1 and subsequent Western blot analysis with an anti-PSTPIP antiserum (which recognizes human and mouse PSTPIP) demonstrated binding of both mouse and human PSTPIP to hFasL. In the input control, several unspecific bands were recognized by the anti-PSTPIP antiserum. *D*, co-immunoprecipitation was performed with 293T cells transiently transfected with *mPSTPIP* in combination with FLAG-tagged versions of full-length *hFasL*, *hFasL* deletion mutants lacking either aa 1–39 ($\Delta 1-39$) or aa 40–80 ($\Delta 40-80$), *hTNF α* , or *mHMGB1*. Input controls demonstrated expression of PSTPIP in the transfected cells. Only full-length and FasL $\Delta 1-39$ efficiently co-immunoprecipitated with PSTPIP, whereas binding of FasL $\Delta 40-80$ to PSTPIP was much reduced. TNF α -FLAG and HMGB1-FLAG served as negative controls.

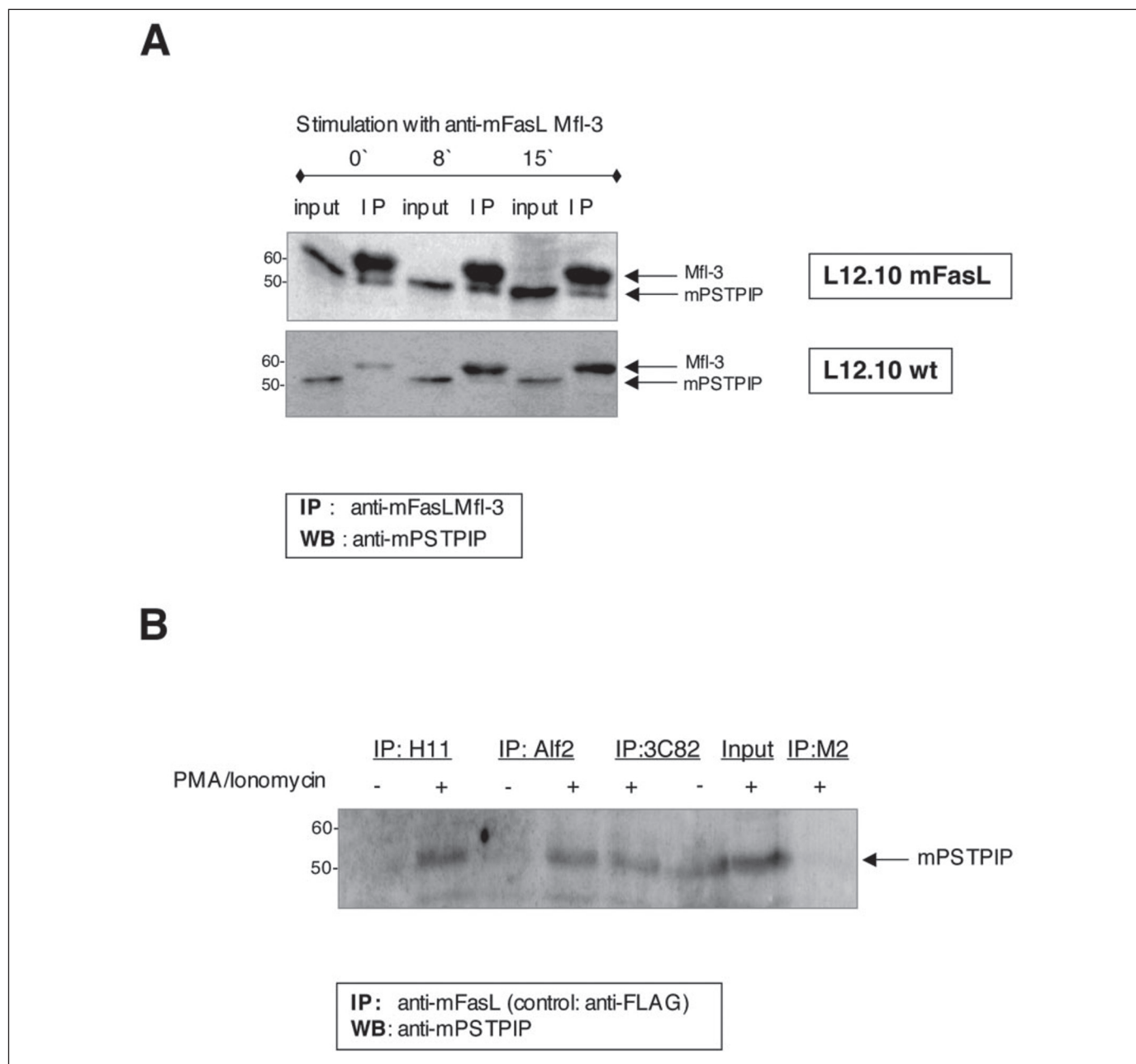


FIGURE 3. Endogenous PSTPIP is co-immunoprecipitated with overexpressed and endogenous FasL in mouse T-cells. *A*, the Fas-resistant mouse thymoma cell line L12.10, stably overexpressing mouse FasL after electroporation with *pBabe-mFasL*, was used for co-immunoprecipitation of endogenous mPSTPIP after activation of FasL by anti-FasL antibody. FasL expression on the surface of the transfected L12.10 cells had been confirmed before by FACS analysis (data not shown). 24-Well plates were coated overnight with biotinylated anti-FasL antibody Mfl-3 (2 $\mu\text{g/ml}$). 5×10^7 L12.10 mFasL or L12.10 wild-type (*wt*) cells were added to the Mfl-3-coated wells for the indicated times. For subsequent immunoprecipitation, cells were lysed, and further biotinylated Mfl-3 antibody was added (1 $\mu\text{g/ml}$). Streptavidin-agarose was employed for precipitation. The figure shows some co-immunoprecipitation of endogenous mPSTPIP with FasL without stimulation of FasL, whereas maximal binding of PSTPIP protein to FasL occurred after 8 min of anti-FasL stimulation. The *IP* lanes display the IgG heavy chain of the Mfl-3 antibody used for precipitation. *B*, 1.5×10^7 mouse splenocytes were either stimulated with 10 ng/ml phorbol 12-myristate 13-acetate and 0.2 $\mu\text{g/ml}$ ionomycin (+) or left untreated (-). After 18 h, the cells were treated for 30 min with the metalloprotease inhibitor phenanthroline (1.5 mM) and then lysed for co-immunoprecipitation with different anti-FasL antibodies (H11 and 3C82 (*Alexis*) and Alf2 (*Ancell*)). All three antibodies were able to co-immunoprecipitate endogenous mPSTPIP with mFasL in stimulated, but not in unstimulated, T-cells, whereas the M2 anti-FLAG antibody did not precipitate detectable amounts of mPSTPIP. Efficiency of FasL precipitation could not be controlled due to the lack of anti-mouse FasL antibodies suitable for Western blot analysis. *IP*, immunoprecipitation; *WB*, Western blot.

tested whether binding of PSTPIP plays a role in FasL sorting. Epithelial 293T cells do not express detectable levels of PSTPIP (25),⁵ and when we transfected *hFasL* into these cells, we could measure profound FasL expression at the cell surface by FACS analysis. However, co-transfection of human or mouse *PSTPIP* decreased the amount of surface FasL significantly (Fig. 5A).

To collect further experimental evidence that the interaction of PSTPIP with the cytoplasmic part of FasL regulates cell surface expression of the ligand, we overexpressed a PSTPIP mutant lacking the SH3 domain together with FasL in RBL 2H3 cells, which normally retain FasL intracellularly (14). The PSTPIP ΔSH3 mutant is still able to interact with other proteins and structures via its N-terminal protein-protein interaction motives, but it is not capable of binding to FasL. Therefore, PSTPIP ΔSH3 is likely to act as a dominant negative PSTPIP mutant with

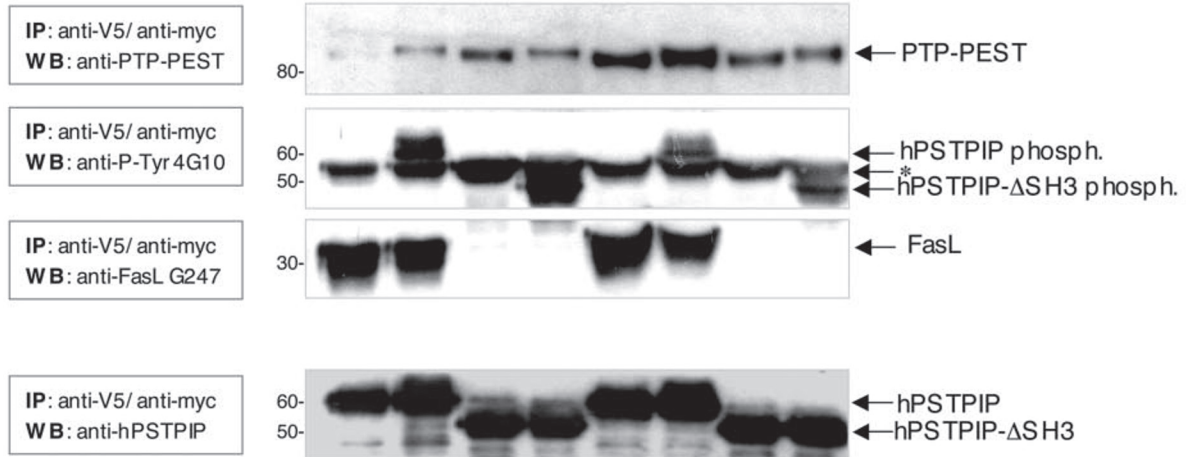
⁵ W. Baum, O. Janssen, and M. Zörnig, unpublished observation.

A

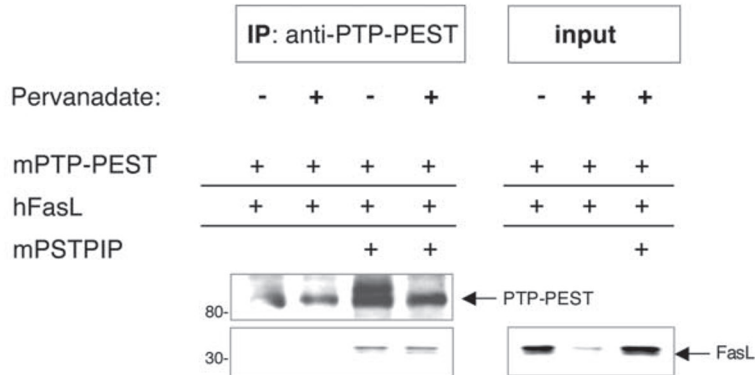
Pervanadate:	-	+	-	+	-	+	-	+
mPTP-PEST					+	+	+	+
hFasL	+	+	+	+	+	+	+	+
hPSTPIP-V5	+	+			+	+		
hPSTPIP ΔSH3-myc			+	+			+	+

hPSTPIP:
IP: anti-V5

hPSTPIP ΔSH3:
IP: anti-myc 9B11



B



C

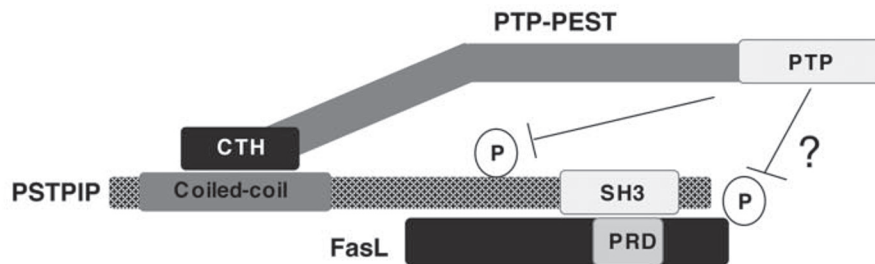


FIGURE 4. FasL, PSTPIP, and PTP-PEST form a ternary complex in which PSTPIP is dephosphorylated. A, COS cells were transfected with *pCR33-FLAG-hFasL*, *PSTPIP* (either V5-tagged full-length *pcDNA3.1-hPSTPIP* or Myc-tagged *pcMV tag3b-hPSTPIP ΔSH3* lacking the *PSTPIP* SH3 domain), and *pcDNA3.1 PTP-PEST* in different combinations. 48 h after transfection, half of the cells were pretreated with pervanadate for 4 h (+). Immunoprecipitations were performed with anti-Myc (for hPSTPIP ΔSH3) or anti-V5 (for full-length hPSTPIP) antibodies. Both antibodies precipitated similar amounts of PSTPIP proteins (see anti-hPSTPIP Western blot). The figure shows that FasL co-precipitates only with full-length hPSTPIP and not with PSTPIP lacking its C-terminal SH3 domain (see anti-FasL Western blot), whereas PTP-PEST was co-precipitated with both forms of PSTPIP (anti-PTP-PEST Western

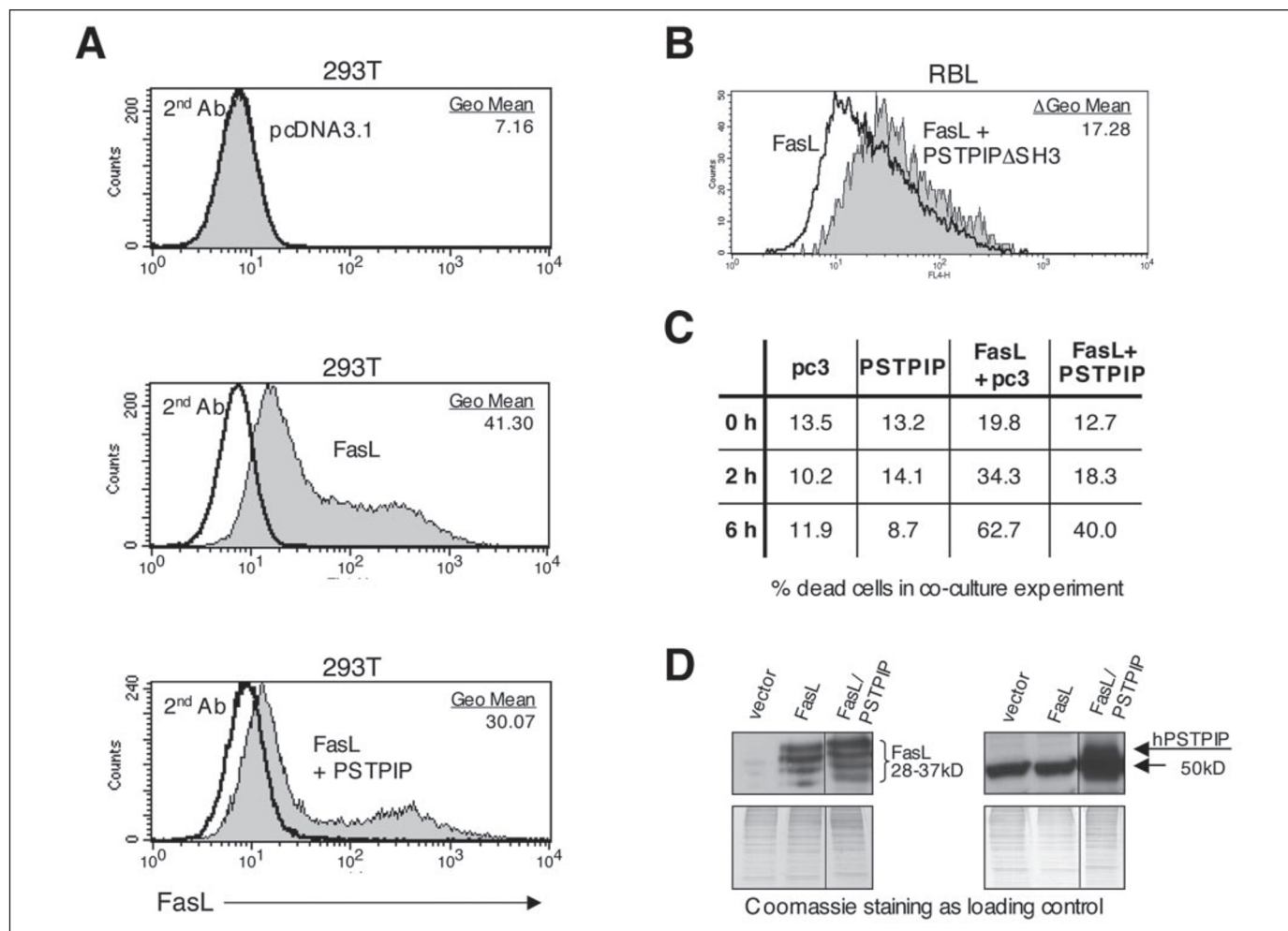


FIGURE 5. Co-expression of PSTPIP decreases FasL cell surface expression and killing capacity in 293T cells. *A*, human FasL (*pcRC33-FLAG-hFasL*) was transfected either alone or together with hPSTPIP (*pcDNA3.1-hPSTPIP*) into 1×10^6 293T cells. 48 h later, cells were stained with anti-FasL antibody (Nok-1) plus anti-mouse secondary antibody coupled to fluorescein isothiocyanate for subsequent FACS analysis. Average FasL cell surface expression was measured as an arbitrary geometrical mean fluorescein isothiocyanate fluorescence. Empty vector (*pcDNA3.1*) transfection and staining only with secondary anti-mouse antibody (*2nd Ab*) served as negative controls. *B*, RBL 2H3 cells were electroporated with full-length *hFasL* together with either empty vector (*thick line*) or with *PSTPIPΔSH3* (lacking the PSTPIP SH3 domain; *thin line with gray filling*). FasL cell surface expression was quantified 24 h later with Nok-1 anti-FasL antibody and APC-coupled anti-mouse secondary antibody by FACS analysis. The increase in FasL cell surface expression upon co-transfection of *PSTPIPΔSH3* was measured as an arbitrary geometrical mean fluorescence shift (Δ Geo Mean). *C*, single and double transfected 293T cells from *A* were used 48 h after transfection for a co-culture killing assay with Fas-sensitive A20 Jurkat target cells. *D*, transfected 293T cells used in *A* and *C* were analyzed by Western blot for total FasL protein expression. G247 antibody was used to detect FasL, and equal loading of lysates was confirmed by Coomassie staining of the gel. Several (glycosylated) FasL bands were detected between 28 and 37 kDa, and co-expression of hPSTPIP did not decrease the overall amount of FasL in the cells. The anti-hPSTPIP serum detected the target protein above an unspecific 50-kDa signal.

respect to its FasL-relevant function(s). Fig. 5*B* demonstrates that co-expression of PSTPIP Δ SH3 increases FasL cell surface expression in comparison with cells that were co-transfected with *FasL* and empty vector.

The decrease of FasL cell surface expression upon co-expression with PSTPIP was confirmed in co-culture experiments when we incubated transfected 293T cells with Fas-sensitive Jurkat target cells. Whereas *FasL*-transfected cells killed 34.3% of target cells after 2 h and 62.7% after 6 h of co-culture, cells transfected with the same amount of *FasL* and with *PSTPIP* killed 18.3 and 40.0% of cells, respectively (Fig. 5*C*). In 14 independent co-culture experiments, we observed a reduction in FasL-

mediated target cell killing of $35.2 \pm 17.6\%$ after PSTPIP co-transfection. This reduction in FasL cell surface expression and FasL-induced target cell death upon PSTPIP co-expression was due to increased intracellular FasL localization and not due to decreased total FasL protein expression, as was seen in Western blot analysis of lysates prepared from the transfected cells (Fig. 5*D*).

To confirm these data and to ensure that cells with equal amounts of total FasL were compared for relative FasL cell surface expression, we used a *hFasL* construct tagged with *GFP* at the cytoplasmic N terminus for transfection experiments. By gating regions of identical GFP fluorescence during FACS analysis, we analyzed cells with similar quantities of

blot; endogenous (*lanes 1–4*) and overexpressed (*lanes 5–8*) PTP-PEST. Moreover, this figure illustrates that PSTPIP is tyrosine-phosphorylated, since the anti-phosphotyrosine antibody 4G10 only detects a specific signal after tyrosine phosphatase inhibition with pervanadate (anti-Tyr(P) 4G10 Western blot; the band marked with an asterisk is nonspecific). Pervanadate treatment also resulted in a small shift of the PTP-PEST signal toward higher molecular weight (compare, for example, *lane 1* with *lane 2*, *lane 3* with *lane 4*, and so on in the anti-PTP-PEST Western blot), indicating that PTP-PEST itself is regulated by phosphorylation, as has been published before (15, 24). *B*, when immunoprecipitation was performed with anti-PTP-PEST in transfected COS cells, co-precipitation of FasL was only observed in the presence of PSTPIP. No differences were observed between pervanadate-treated and untreated cells. These data confirm that FasL and PTP-PEST form a ternary complex *in vivo* by binding to different regions of the adaptor protein PSTPIP, as shown schematically in *C*. In this complex, PSTPIP is dephosphorylated, most likely by PTP-PEST, which may also influence FasL phosphorylation. *IP*, immunoprecipitation; *WB*, Western blot.

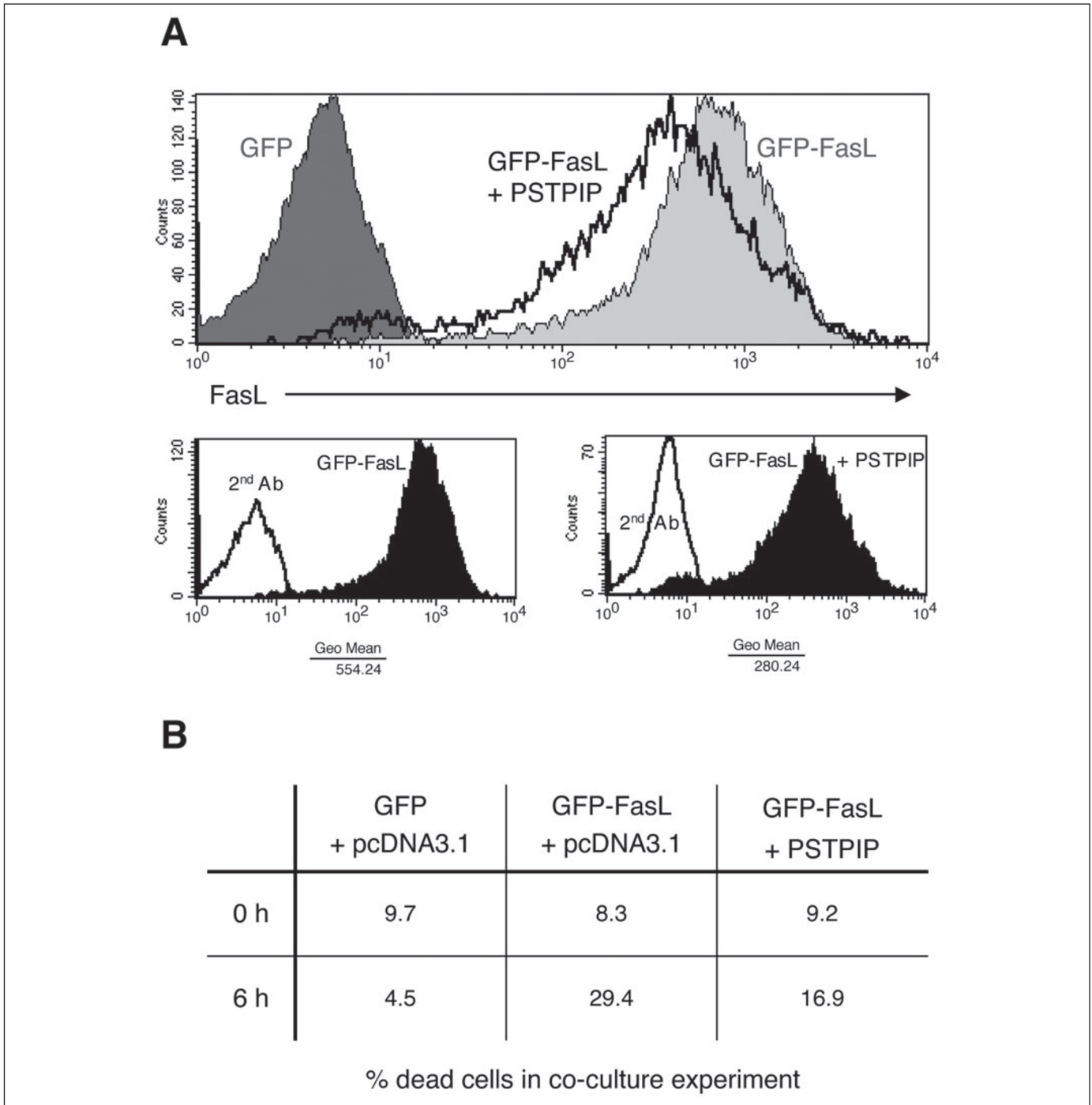


FIGURE 6. GFP-FasL cell surface expression and its killing capacity are decreased upon PSTPIP co-transfection. *A*, *hFasL* with an N-terminal GFP-tag was transfected alone or with *hPSTPIP*. 48 h later, cells with similar GFP fluorescence, and therefore equal amounts of GFP-FasL, were gated during FACS analysis in the FL1 channel and analyzed for FasL surface expression by staining with the anti-FasL antibody Nok-1 and anti-mouse secondary antibody coupled to APC (2nd Ab). Staining with anti-mouse antibody alone served as a negative control. The top histogram shows an overlay of cells transfected with GFP vector control (GFP) and cells transfected with GFP-FasL alone (GFP-FasL) or in combination with PSTPIP (GFP-FasL + PSTPIP). The histograms below were used to quantify the average FasL surface expression as the arbitrary geometrical fluorescence of GFP-FasL-transfected cells (left) and of cells transfected with GFP-FasL plus PSTPIP (right). *B*, a co-culture assay was performed using the transfected target cells from *A* with Fas-sensitive A20 Jurkat target cells.

total FasL protein (which we again confirmed by Western blot; data not shown). FACS measurement of cell surface FasL with the anti-FasL antibody Nok-1 once more revealed a decrease in membrane-anchored FasL and consequently an increased proportion of intracellular FasL within the PSTPIP-co-transfected cells (Fig. 6A). The reduction in surface FasL upon co-expression of PSTPIP was validated by decreased killing rates in co-culture experiments (Fig. 6B). The specificity of PSTPIP in its ability to relocalize FasL from the cell surface to the cytoplasm

was supported by control transfections with *XIAP* and *HMGB1* (high mobility group box 1) cDNAs, which code for cytoplasmic proteins. Their co-expression with FasL did not influence cell surface staining and killing activity of the ligand in co-culture assays (data not shown). Importantly, co-transfection of *CD34*, another human cell surface molecule, together with *hPSTPIP* did not change *CD34* surface expression when compared with *CD34* single transfected cells (data not shown). These findings demonstrate that the FasL-binding protein PSTPIP is

PSTPIP and Intracellular FasL Localization

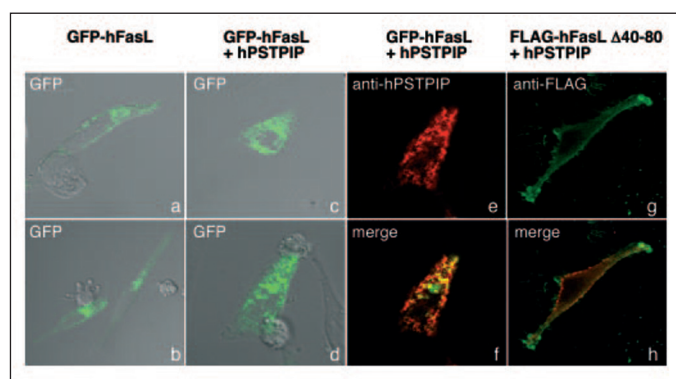


FIGURE 7. Localization studies in HeLa cells reveal decreased cell surface expression and increased intracellular storage of FasL upon co-transfection with PSTPIP. HeLa cells were transfected by electroporation with *GFP-hFasL* alone or in combination with Myc-tagged *hPSTPIP*, grown on coverslips for 24 h, and then used for immunostaining with anti-Myc antibody, followed by anti-mouse *Alexa546*. *a* and *b* show single transfected *GFP-hFasL*-expressing cells; *c* and *d* show cells expressing *GFP-hFasL* plus *hPSTPIP*. Overlays of the GFP fluorescence and normal transmission images are shown. *e* displays the localization of *hPSTPIP* in the cell shown in *d*, and *f* illustrates the overlay of *GFP-hFasL* and *PSTPIP* within this cell, whereby the yellow color demonstrates co-localization of both proteins. In *g* and *h*, FLAG-tagged *hFasL* $\Delta 40-80$ (lacking the intracellular proline-rich region) was co-transfected with *hPSTPIP*, and for detection, M2 anti-FLAG antibody and anti-PSTPIP antiserum were used. In contrast to the full-length protein (*e* and *f*), the $\Delta 40-80$ FasL mutant does not co-localize with *PSTPIP*.

involved in the storage of FasL in intracellular compartments, a result that we could support by localization studies with HeLa cells using confocal laser-scanning microscopy (Fig. 7). Whereas single transfection of GFP-tagged *hFasL* led to predominantly cell surface expression of the molecule (Fig. 7, *a* and *b*), co-transfection of *FasL* with *hPSTPIP* resulted in the expected co-localization of both proteins and the retention of FasL in intracellular vesicles (Fig. 7, *c-f*).

DISCUSSION

The Fas Ligand molecule is well known for its capacity to induce apoptosis by activating the corresponding death receptor Fas (27). However, its highly conserved 80-aa-long cytoplasmic domain contains several prominent signaling motifs, which argues for the existence of a reverse signaling mechanism via FasL into the ligand-bearing cell (1, 2, 6, 12). In addition, the cytoplasmic domain has been implicated in FasL sorting in hematopoietic cells to specialized intracellular organelles, the secretory lysosomes (13). Cellular proteins interacting with the intracellular FasL domain may also influence the capability of the ligand to induce apoptosis by Fas receptor activation, for example by preventing oligomerization of FasL. So far, the molecules that bind to the intracellular FasL domain and are responsible for such aspects of FasL biology have not been functionally characterized, although different proteins have been suggested as FasL-interacting proteins (28, 29).

In this study, we show by a number of methods that the adaptor protein PSTPIP binds to the intracellular FasL domain. We confirmed our initial yeast two-hybrid result by *in vitro* GST pull-down, co-immunoprecipitation of overexpressed and endogenous proteins, and co-localization. PSTPIP is a homolog of *Schizosaccharomyces pombe* CDC15p, a protein involved in the assembly of the actin ring in the cytokinetic cleavage furrow (15). Mouse PSTPIP has been identified as an interactor of the PEST-type protein-tyrosine phosphatase PTP-HSCF (15), and human PSTPIP has been found to interact with the CD2 cytoplasmic domain and to down-regulate CD2-stimulated T-cell adhesion through coupling of the protein-tyrosine phosphatase PTP-PEST to CD2 (16). PSTPIP belongs to a family of structurally related proteins characterized by a similar modular composition of an N-terminal FCH (Fes/CIP4 homology) domain, followed by a coiled-coil region and a

C-terminal SH3 domain (FCH/SH3 protein family). Our experiments show that PSTPIP interacts with the N-terminal proline-rich domain within FasL via its SH3 domain. We also demonstrate that co-transfection of *PSTPIP* with *FasL* decreases cell surface FasL expression, whereas the amount of intracellular FasL is enlarged, arguing that the interaction of PSTPIP with FasL is important for intracellular sorting of FasL.

PSTPIP is able to bind to the phosphatase PTP-PEST via its coiled-coil domain (16, 24–26), and we could prove the existence of a trimeric complex consisting of FasL, PSTPIP, and PTP-PEST by co-immunoprecipitation experiments.

Interaction with the PSTPIP SH3 domain has not only been reported for CD2, but also for the Wiskott-Aldrich syndrome protein WASP and for the c-Abl kinase. PSTPIP serves as a scaffold protein between PTP-PEST and WASP, allowing the phosphatase to dephosphorylate WASP and thereby inhibit WASP-driven actin polymerization and formation of the immunological synapse (25, 26). PSTPIP also directs PTP-PEST to the c-Abl kinase to mediate Abl dephosphorylation and inactivation (24). The data on PSTPIP interactions with CD2 and WASP and its homology to yeast CDC15p suggest a role for PSTPIP in the organization of the cytoskeleton. Recently, mutations in human PSTPIP that disrupt binding to PTP-PEST have been linked to PAPA syndrome, an autoinflammatory disorder (30). Further interactions of PSTPIP with CD4, CD8, CD54, and CD62L have been published, the functional roles of which remain to be established (20).

Our experiments reveal that binding of PSTPIP to the intracellular domain of FasL influences the localization of the ligand within the cell. In T- and NK-cells, FasL is targeted to specialized secretory lysosomes, which fuse with the plasma membrane upon recognition of a target cell (13, 14). These Golgi-derived vesicles carry lysosomal markers (e.g. lysosome-associated membrane proteins), and, apart from FasL, they contain other cytolytic effector molecules including perforins and granzymes. Storage of newly synthesized FasL ensures that the ligand appears on the cell surface only upon activation and precisely at the contact site between effector and target cell (immunological synapse), thereby preventing nonspecific killing by T- and NK-cells. In nonhematopoietic cells with conventional lysosomes, however, FasL appears directly on the plasma membrane. FasL is targeted to secretory lysosomes via the proline-rich domain in its cytoplasmic tail, between aa 40 and 70, and it has been speculated that an interaction of this domain with an SH3 domain-containing protein might facilitate direct sorting of FasL to secretory lysosomes (14). We could show that PSTPIP binds to the proline-rich domain of FasL via its SH3 domain and that co-transfection of PSTPIP with FasL into nonhematopoietic cells decreases the amount of cell surface FasL and increases its storage in intracellular granules. PSTPIP is a promising candidate for FasL sorting to secretory lysosomes, since its expression is limited to hematopoietic cells, namely T- and NK-cells (15, 16), which contain the secretory lysosomes used for intracellular FasL storage (13, 14).

Several members of the FCH/SH3 protein family have been functionally linked to the cytoskeleton and to endocytosis. In particular, FBP17 (formin-binding protein 17) has been shown to interact with dynamin and to regulate endocytosis by forming vesicotubular structures (31). PSTPIP, on the other hand, is involved in actin polymerization (32), a process known to be important for endocytosis (33). One could speculate that co-expression of PSTPIP with FasL leads to decreased FasL cell surface expression because of a PSTPIP-induced increase in endocytosis. However, such an explanation is not plausible in the light of our observation that the level of cell surface expression of another receptor, hCD34, is not influenced by co-expression of PSTPIP.

Reverse signaling into the ligand-bearing cell has been described for several members of the TNF family. So far, this bidirectional signaling capacity has been associated with 6 of 16 TNF family members (CD27L, CD30L, CD40L, CD137L, TNF α , and FasL) that contain a putative casein kinase I (CKI) substrate motive (for a review, see Ref. 2), although CKI-dependent serine phosphorylation upon receptor activation has, until now, only been shown for TNF α (11). Studies with primary T-cells from wild-type mice and animals defective for FasL (*gld*) or Fas (*lpr*) have suggested that FasL influences the proliferative behavior of T-cells (7–9).⁶ Furthermore, an increase in Erk1/2 phosphorylation and activation of the cytosolic phospholipase A2 have been reported for the mouse-derived Sertoli cell line TM4 after cross-linking of endogenous FasL with antibodies (10). In our own experiments, we observed an increase in Erk1/2 phosphorylation in *FasL*-transfected 293T cells upon stimulation with the anti-FasL antibody Nok-1 as well as an increase in p38-mitogen-activated protein kinase phosphorylation after treatment of the same cells with a soluble Fas receptor molecule (Fas-Fc), which binds to surface FasL (data not shown). Such reverse signaling events may also depend on the proline-rich domain within the cytoplasmic part of FasL and on recruitment of a SH3 domain-containing protein like PSTPIP. PSTPIP is able to bind to the protein-tyrosine phosphatases PTP-HSCF and PTP-PEST as an adaptor protein and to recruit them to other target proteins (15, 16). Trimeric complexes of PSTPIP and PTP-PEST with the kinase *c-Abl* or the WASP protein have so far been described (24–26). In such complexes, PTP-PEST dephosphorylates both the adaptor protein PSTPIP and the PSTPIP-binding protein, either *c-Abl* or WASP. Whereas the phosphorylation status of PSTPIP may influence its capability to interact with its binding partners (18), dephosphorylation of *c-Abl* and WASP by PTP-PEST deactivates these proteins. In overexpression studies, we could demonstrate the existence of FasL-PSTPIP-PTP-PEST complexes in COS cells. Whereas the proline-rich domain of FasL interacts with the PSTPIP SH3 domain, PTP-PEST binds independently to the N-terminal PSTPIP coiled-coil stretch via its C-terminal CTH domain (19, 25). To what extent the PSTPIP-PTP-PEST-FasL complex formation is influencing the other aggregates of PSTPIP-PTP-PEST with *c-Abl* or WASP (or whether it is regulated itself by such complexes) will be a matter of future studies. In accordance with published data, we could demonstrate that tyrosine-phosphorylated PSTPIP is dephosphorylated by the interacting PTP-PEST phosphatase (25, 34). Nevertheless, we could not show tyrosine phosphorylation of FasL upon phosphatase inhibition in COS cells, which may be due to the absence of FasL kinases or to inefficient PTP-PEST inactivation. The latter speculation is supported by the fact that, in our experiments, overexpression of PTP-PEST led to decreased PSTPIP phosphorylation even in the presence of pervanadate. In essence, our data suggest that binding of PSTPIP and PTP-PEST may influence the phosphorylation status of FasL in relevant cell types, such as T-cells, which express endogenous PSTPIP and PTP-PEST proteins (25) and in which reverse signaling via FasL has been shown to influence activation-induced proliferation (7–9). It is interesting to note that we observed an increase in endogenous PSTPIP recruitment to overexpressed cell surface FasL in mouse thymoma cells upon stimulation of the ligand with soluble Fas receptor. Such recruitment of PSTPIP to stimulated membrane-bound FasL might indicate a further role for PSTPIP (and PTP-PEST) in the regulation of cell surface FasL and/or FasL reverse signaling in T-cells, which express the endogenous PSTPIP protein.

FasL is a very dangerous molecule for a cell to display at the cell surface due to its potent ability to induce cell death. Therefore, the

protein is expressed in only a few cells and is regulated at different levels. The *FasL* gene contains binding sites for several transcription factors and has been reported to be transcriptionally up-regulated by, for example, NF- κ B, *c-Myc*, RAR γ , Nur77, *c-Jun/FosB* (AP-1), Sp1, Egr1/2/3, NF-AT (35) in activated T-cells. Its localization within intracellular organelles in T- and NK-cells, followed by a controlled delivery to the immunological synapse upon activation, ensures that only the recognized target cell is killed (13, 14). FasL surface expression is then down-regulated by matrix metalloproteases, which cleave the extracellular FasL domain (36–39). However, some cells release apoptosis-inducing full-length FasL in microvesicles into their environment (40–42). Therefore, proteolysis and exocytosis are also involved in FasL regulation. In addition, we have observed FasL localization of FasL in lipid rafts at the cell surface,⁷ which further influences localization, stability, and the cell death-inducing capacity of the molecule. The sheer number of regulatory levels indicates a complex interdependence and interplay of these processes, which are likely to involve several different interacting proteins. With PSTPIP, we have identified a molecule that binds to the intracellular FasL domain and is involved in at least one of these regulatory processes, namely localization. In addition, by forming a trimeric complex with FasL and the phosphatase PTP-PEST, PSTPIP is likely to be implicated in the regulation of FasL phosphorylation and possibly in an additional reverse signaling role of FasL. Future studies, including analysis of knockout/knockin mouse models in which the wild-type *FasL* allele has been replaced by a deletion mutant lacking the intracellular domain, will help to elucidate the consequences of PSTPIP binding to FasL and the physiological role of FasL reverse signaling.

Acknowledgments—We thank Laurence Lasky and Susan Spencer (Department of Molecular Oncology, Genentech, Inc., South San Francisco, CA) for mouse PSTPIP cDNA and antiserum, Carol Wise for human PSTPIP/CD2BP1 cDNA constructs and antiserum, Nicholas Tonks for the PTP-PEST cDNA and antiserum, Hermann Eibel (Clinical Research Unit for Rheumatology, Freiburg, Germany) for several human FasL constructs, and Jürg Tschopp (Department of Biochemistry, University of Lausanne, Switzerland) for stably transfected 293 cells (293-005).

REFERENCES

- Janssen, O., Qian, J., Linkermann, A., and Kabelitz, D. (2003) *Cell Death Differ.* **10**, 1215–1225
- Linkermann, A., Qian, J., and Janssen, O. (2003) *Biochem. Pharmacol.* **66**, 1417–1426
- Holler, N., Tardivel, A., Kovacovics-Bankowski, M., Hertig, S., Gaide, O., Martinon, F., Tinel, A., Deperthes, D., Calderara, S., Schulthess, T., Engel, J., Schneider, P., and Tschopp, J. (2003) *Mol. Cell Biol.* **23**, 1428–1440
- Nagata, S. (1994) *Adv. Immunol.* **57**, 129–144
- Muzio, M., Chinnaiyan, A. M., Kischkel, F. C., O'Rourke, K., Shevchenko, A., Ni, J., Scaffidi, C., Bretz, J. D., Zhang, M., Gentz, R., Mann, M., Krammer, P. H., Peter, M. E., and Dixit, V. M. (1996) *Cell* **85**, 817–827
- Newell, M. K., and Desbarats, J. (1999) *Apoptosis* **4**, 311–315
- Suzuki, I., and Fink, P. J. (1998) *J. Exp. Med.* **187**, 123–128
- Suzuki, I., Martin, S., Boursalian, T. E., Beers, C., and Fink, P. J. (2000) *J. Immunol.* **165**, 5537–5543
- Desbarats, J., Duke, R. C., and Newell, M. K. (1998) *Nat. Med.* **4**, 1377–1382
- Ulisse, S., Cinque, B., Silvano, G., Rucci, N., Biordi, L., Cifone, M. G., and D'Armiento, M. (2000) *Cell Death Differ.* **7**, 916–924
- Watts, A. D., Hunt, N. H., Wanigasekara, Y., Bloomfield, G., Wallach, D., Roufogalis, B. D., and Chaudhri, G. (1999) *EMBO J.* **18**, 2119–2126
- Takahashi, T., Tanaka, M., Inazawa, J., Abe, T., Suda, T., and Nagata, S. (1994) *Int. Immunol.* **6**, 1567–1574
- Blott, E. J., and Griffiths, G. M. (2002) *Nat. Rev. Mol. Cell Biol.* **3**, 122–131
- Blott, E. J., Bossi, G., Clark, R., Zvelebil, M., and Griffiths, G. M. (2001) *J. Cell Sci.* **114**, 2405–2416

⁶ W. Baum and M. Zörnig, unpublished data.

⁷ N. Cahzac, W. Baum, V. Kirkin, F. Conchonaud, L. Wawrezynieck, D. Marguet, O. Janssen, M. Zörnig, and A.-O. Hueber, manuscript in preparation.

PSTPIP and Intracellular FasL Localization

15. Spencer, S., Dowbenko, D., Cheng, J., Li, W., Brush, J., Utzig, S., Simanis, V., and Lasky, L. A. (1997) *J. Cell Biol.* **138**, 845–860
16. Li, J., Nishizawa, K., An, W., Hussey, R. E., Lialios, F. E., Salgia, R., Sunder-Plassmann, R., and Reinherz, E. L. (1998) *EMBO J.* **17**, 7320–7336
17. Fields, S., and Song, O. (1989) *Nature* **340**, 245–246
18. Wu, Y., Spencer, S. D., and Lasky, L. A. (1998) *J. Biol. Chem.* **273**, 5765–5770
19. Dowbenko, D., Spencer, S., Quan, C., and Lasky, L. A. (1998) *J. Biol. Chem.* **273**, 989–996
20. Bai, Y., Ding, Y., Spencer, S., Lasky, L. A., and Bromberg, J. S. (2001) *Exp. Mol. Pathol.* **71**, 115–124
21. Brunner, T., Mogil, R. J., LaFace, D., Yoo, N. J., Mahboubi, A., Echeverri, F., Martin, S. J., Force, W. R., Lynch, D. H., and Ware, C. F. (1995) *Nature* **373**, 441–444
22. Ju, S. T., Panka, D. J., Cui, H., Ettinger, R., el-Khatib, M., Sherr, D. H., Stanger, B. Z., and Marshak-Rothstein, A. (1995) *Nature* **373**, 444–448
23. Yang, Y., Mercep, M., Ware, C. F., and Ashwell, J. D. (1995) *J. Exp. Med.* **181**, 1673–1682
24. Cong, F., Spencer, S., Cote, J. F., Wu, Y., Tremblay, M. L., Lasky, L. A., and Goff, S. P. (2000) *Mol. Cell* **6**, 1413–1423
25. Cote, J. F., Chung, P. L., Theberge, J. F., Halle, M., Spencer, S., Lasky, L. A., and Tremblay, M. L. (2002) *J. Biol. Chem.* **277**, 2973–2986
26. Badour, K., Zhang, J., Shi, F., Leng, Y., Collins, M., and Siminovitch, K. A. (2004) *J. Exp. Med.* **199**, 99–112
27. Thorburn, A. (2004) *Cell. Signal.* **16**, 139–144
28. Ghadimi, M. P., Sanzenbacher, R., Thiede, B., Wenzel, J., Jing, Q., Plomann, M., Borkhardt, A., Kabelitz, D., and Janssen, O. (2002) *FEBS Lett.* **519**, 50–58
29. Hane, M., Lowin, B., Peitsch, M., Becker, K., and Tschopp, J. (1995) *FEBS Lett.* **373**, 265–268
30. Wise, C. A., Gillum, J. D., Seidman, C. E., Lindor, N. M., Veile, R., Bashiardes, S., and Lovett, M. (2002) *Hum. Mol. Genet.* **11**, 961–969
31. Kamioka, Y., Fukuhara, S., Sawa, H., Nagashima, K., Masuda, M., Matsuda, M., and Mochizuki, N. (2004) *J. Biol. Chem.* **279**, 40091–40099
32. Badour, K., Zhang, J., Shi, F., McGavin, M. K., Rampersad, V., Hardy, L. A., Field, D., and Siminovitch, K. A. (2003) *Immunity* **18**, 141–154
33. Merrifield, C. J. (2004) *Trends Cell Biol.* **14**, 352–358
34. Angers-Loustau, A., Cote, J. F., Charest, A., Dowbenko, D., Spencer, S., Lasky, L. A., and Tremblay, M. L. (1999) *J. Cell Biol.* **144**, 1019–1031
35. Li-Weber, M., and Krammer, P. H. (2003) *Semin. Immunol.* **15**, 145–157
36. Tanaka, M., Itai, T., Adachi, M., and Nagata, S. (1998) *Nat. Med.* **4**, 31–36
37. Knox, P. G., Milner, A. E., Green, N. K., Eliopoulos, A. G., and Young, L. S. (2003) *J. Immunol.* **170**, 677–685
38. Schneider, P., Holler, N., Bodmer, J. L., Hahne, M., Frei, K., Fontana, A., and Tschopp, J. (1998) *J. Exp. Med.* **187**, 1205–1213
39. Hallermalm, K., De Geer, A., Kiessling, R., Levitsky, V., and Levitskaya, J. (2004) *Cancer Res.* **64**, 6775–6782
40. Martinez-Lorenzo, M. J., Anel, A., Gamen, S., Monlen, I., Lasierra, P., Larrad, L., Pineiro, A., Alava, M. A., and Naval, J. (1999) *J. Immunol.* **163**, 1274–1281
41. Jodo, S., Xiao, S., Hohlbaum, A., Strehlow, D., Marshak-Rothstein, A., and Ju, S. T. (2001) *J. Biol. Chem.* **276**, 39938–39944
42. Martinez-Lorenzo, M. J., Anel, A., Alava, M. A., Pineiro, A., Naval, J., Lasierra, P., and Larrad, L. (2004) *Exp. Cell Res.* **295**, 315–329
43. Bartel, P. L., and Fields, S. (1995) *Methods Enzymol.* **254**, 241–263